

## Melting transitions of monolayers adsorbed in cylindrical nanopores

L. FIRLEJ<sup>1\*</sup>, B. KUČHTA<sup>2</sup>

<sup>1</sup>Laboratoire des Colloïdes, Verres, Nanomatériaux (LCVN),  
Université Montpellier II, 34095, Montpellier, France

<sup>2</sup>Laboratoire des Matériaux Divisés, Revêtement, Electrocéramiques (MADIREL),  
Université de Provence, Centre de Saint-Jérôme, 13397 Marseille, France

Melting of krypton layers adsorbed in models of MCM-41 porous silica and of carbon nanotubes has been simulated using Monte Carlo methods. We have shown that the melting mechanism depends on the strength of the atom-wall interaction and on the number of layers adsorbed in the pore. Every new layer stabilizes the layers already present in the system. In the carbon nanotubes we found that adsorption of the second layer leads to a freezing of the first one at constant temperature.

Key words: *porous material; melting; freezing; Monte Carlo simulations*

### 1. Introduction

Studies of melting and freezing in confined geometry are of practical relevance to such areas as weathering of rocks, frost heaving, oil industry, properties of porous media and many others. A number of developments resulted in finding the field interesting from a fundamental point of view. Many novel structures with quasi-ideal, isolated cylindrical or slit-shaped pores of nanometric size are now available. Experiments performed on these model porous materials show a melting point elevation in narrow pores, in contrast to the almost universally observed depression of transition temperature in larger pores. In some cases the mechanism of transitions appears to be fundamentally different from those observed in bulk materials.

The influence of the confinement on the solid-liquid transition follows directly from the fact that if a liquid wets the walls in the presence of the solid phase, the liquid will be thermodynamically favoured in confinement. As a consequence, a lower-

---

\*Corresponding author, e-mail: firlej@LCVN.univ-montp2.fr

ing of the melting temperature will be observed. The quantitative dependence of melting (freezing) point depression  $\Delta T = T_b - T_p$  resulting from the Clausius–Clapeyron equation has the form [1]:

$$\Delta T = -\frac{T_b}{\Delta H} \frac{2}{r} [V_l \gamma_l - V_s \gamma_s] \quad (1)$$

where  $T_b$  is the bulk melting temperature,  $T_p$  – melting temperature in a pore of a radius  $r$ ,  $\Delta H$  is the enthalpy of melting,  $V_l$  and  $V_s$  – molar volumes of liquid and solid phases, respectively, and  $\gamma_l$  and  $\gamma_s$  the corresponding surface energies.

The above model of capillary melting is based on simple thermodynamics, without any reference to the molecular nature of the phase. Interactions between the pore wall and the confined particles are taken into account only as surface energy terms  $\gamma_l$  and  $\gamma_s$ . Such a simplification is obviously very restrictive and neglects many important factors that may affect the mechanism of melting [2–8]: various possible structures of the bulk solid, explicit structure of the pore walls, or more complex aspects such as epitaxy, lattice mismatch, crystalline defects, etc. The smaller the pore size, the more serious will be consequences of neglecting the detailed structure of the solid-surface interface. In fact, the structure of a confined solid phase may be different from that of the corresponding bulk phase existing at the same temperature, even for relatively large pore diameters. Additionally, the structure of the solid may vary with the distance from the wall. In other words, the confined phase may be heterogeneous in the vicinity of pore walls. In nanometric pores this effect may concern the whole pore volume.

In this paper, we analyse the mechanism of melting of layers adsorbed in cylindrical nanopores. Our interest has been focused on two factors which may modify the character of melting: the strength of the atom–wall interaction and a corrugation of the wall. The model system is an isolated pore of the diameter of  $d = 4$  nm with krypton gas as the adsorbate. Two situations are analysed. The first one consists of a pore with only one layer adsorbed before the capillary condensation occurs. In this case, the adsorbent–pore wall interaction parameters have been chosen to mimic MCM-41 porous silica. The second situation represents a hypothetical carbon nanotube. In this case, for the same Kr adsorbate, one finds that two Kr layers can be adsorbed before the capillary condensation takes place. This fact is a consequence of stronger adsorbate atom–wall interactions in carbon nanotubes than those in the silica based material. In real systems, the walls of both silica and carbon pores are corrugated. In the case of silica pores, however, the structure of the walls is amorphous, whereas in carbon nanotubes the graphite-like wall is regular and ordered. This difference results in a distribution of adsorption sites which is random and quasi-continuous in silica pores, and regular and discrete in carbon nanotubes. As a consequence, at least to a first approximation, a silica pore can be modelled by a smooth cylinder with an azimuthally non-resolved strength of atom–wall interaction; we used this approach in

this paper. On the contrary, carbon nanotubes were represented by their explicit atomic structure.

In Monte Carlo simulations presented here, the grand canonical ensemble (GCMC) has been used. When atoms have been confined in closed pores, the canonical ensemble (CMC) has been used. The simulation box, containing one pore (with periodic boundary conditions along the tube axis) was assumed to be in equilibrium with the bulk gas obeying the ideal gas law. Trial moves included translations of atoms, insertion of new atoms and removal of existing ones. The system typically contained from 600 to 1300 adsorbed atoms in the box. Typical runs consisted of at least  $10^6$  MC steps per atom. The main results were extracted from previously equilibrated runs.

The Kr–Kr interaction was modelled by the Lennard–Jones (LJ) potential

$$V(r) = 4\epsilon \left( \left( \frac{\sigma}{r} \right)^{12} - \left( \frac{\sigma}{r} \right)^6 \right) \quad (2)$$

with the standard interaction parameters:  $\epsilon_{\text{Kr-Kr}}/k = 171.0$  K,  $\sigma_{\text{Kr-Kr}} = 0.360$  nm. The Kr–nanotube wall interaction was computed by a pair-wise summation of LJ potential (with the LJ parameters for Kr–C interaction obtained from Lorentz–Berthelot mixing rules taking  $\epsilon_{\text{C-C}}/k = 28.0$  K,  $\sigma_{\text{C-C}} = 0.34$  nm). All interactions were calculated within a cutoff radius of 15 Å. Details of the Kr–silica wall interaction are given in [9].

## 2. Melting of a layer on a curved smooth surface

Figure 1 presents four isotherms of krypton adsorption in a smooth silica-like pore. Obviously, their character changes with temperature. Only at the lowest temperature presented here (77 K), the isotherm exhibits a very sharp formation of the first layer. As the temperature increases, the adsorption becomes more continuous, i.e., situations intermediate between a 2D gas and a monolayer are stabilized in the system. Thermodynamically, this is a consequence of increasing entropy of the adsorbed atoms stabilizing these disordered structures. One may speculate, however, that the evolution of the isotherm may also involve some structural changes. To follow this evolution in function of temperature we analyzed the structure of the adsorbed layer along a path corresponding to a constant reduced pressure  $p/p_{\text{cond}} = 0.70$  ( $p_{\text{cond}}$  is the condensation pressure at a given temperature). This choice corresponds to thermodynamic conditions at which the first layer is already well defined and the capillary condensation is not expected yet. It is important to remember that the constant reduced pressure defines different real pressures at different temperatures because the condensation pressure is strongly temperature dependent.

Structural properties of a planar atomic layer are usually represented by parameters sensitive to the deformation of the ideal triangular plane structure. The calcula-

tion of such a parameter in the case of cylindrical surface requires its unfolding into a plane layer. Then, one can apply the order parameter  $\Phi_6$  defined by Mermin [10]:

$$\Phi_6 = \left| \frac{1}{N_b} \sum_{k=1}^{N_b} \exp(i6\theta_k) \right| \quad (3)$$

$\Phi_6$  measures the average bond order within a plane triangular atomic layer. Each nearest neighbouring bond has a particular orientation in the plane that can be described by the polar coordinate  $\theta_k$ . The index  $k$  runs over the total number of nearest neighbour bonds  $N_b$  in the adsorbed layer. One expects that  $\Phi_6 = 1$  in an ideal solid 2D hexagonal crystal and  $\Phi_6 = 0$  when the state of adsorbed layer corresponds to a two-dimensional fluid.

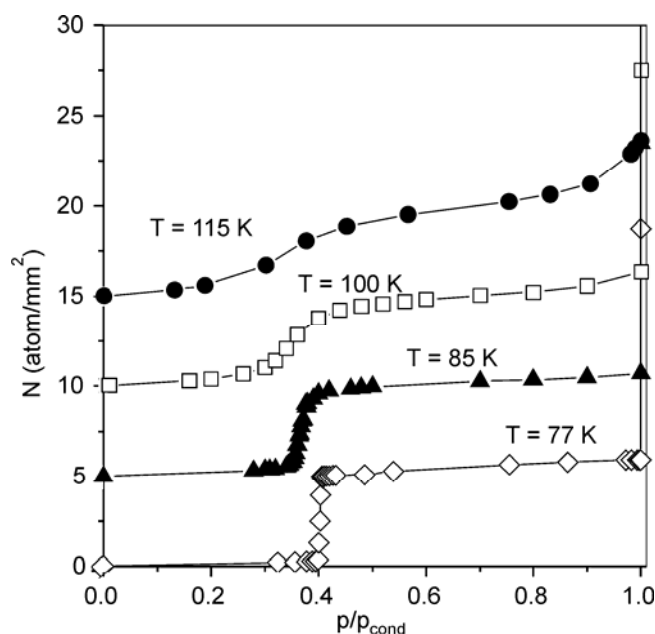


Fig. 1. Adsorption isotherms of Kr in MCM-41 model system. The mean number of adsorbed atoms is drawn as a function of the reduced pressure  $p/p_{\text{cond}}$ , where  $p_{\text{cond}}$  is the capillary condensation pressure at a given temperature. In our case,  $p_{\text{cond}}(77 \text{ K}) = 0.93 \text{ mbar}$ ,  $p_{\text{cond}}(85 \text{ K}) = 5 \text{ mbar}$ ,  $p_{\text{cond}}(100 \text{ K}) = 50 \text{ mbar}$ ,  $p_{\text{cond}}(115 \text{ K}) = 265 \text{ mbar}$ . For clarity, each higher temperature isotherm is shifted by 5 atoms/nm<sup>2</sup> with respect to the previous one

Figure 2 shows the parameter  $\Phi_6$  as a function of temperature, calculated along two thermodynamic paths. First, using the GCMC simulations we followed the path defined by the pressures corresponding to adsorbed and stable monolayer ( $p/p_{\text{cond}} \approx 0.7$ , as described above). This path corresponds to melting in an open system, where the pore is in equilibrium with the external gas. We also followed another path, corresponding to a closed pore. This simulation was performed in the NVT canonical en-

semble. The number of atoms  $N$  was set to be equal to their mean atom number in a monolayer adsorbed at 77 K. A comparison of these two results emphasizes a different mechanism of transformations at each thermodynamic condition.

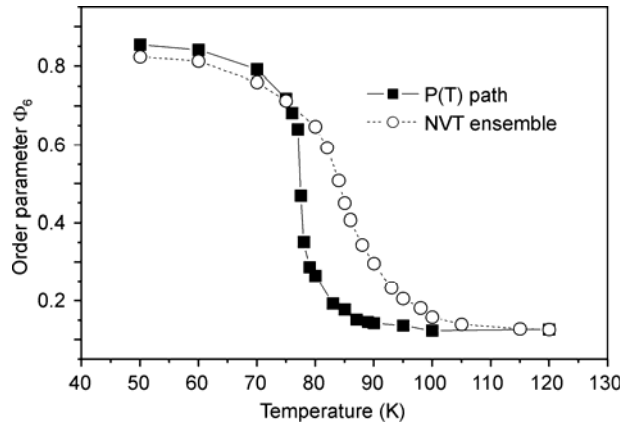


Fig. 2. Order parameter  $\Phi_6$  of Kr monolayer in an open (grand canonical MC simulations along the P-T path, see text) and in closed (canonical MC simulations) MCM-41 pore

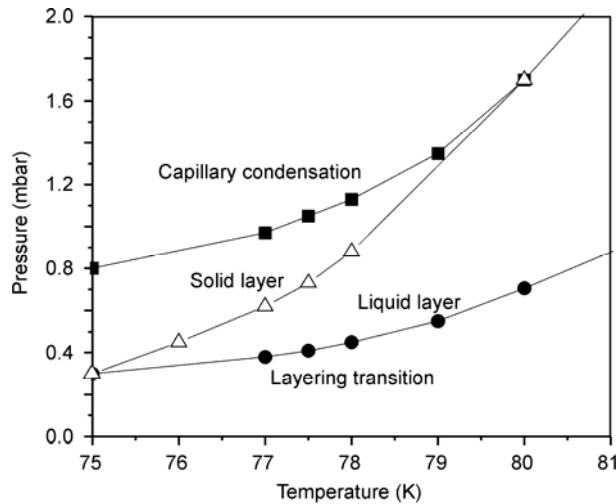


Fig. 3. Phase diagram of krypton adsorbed in a smooth silica-like pore. The equilibrium line between solid and liquid monolayer phase is indicated

First of all, the transition between solid and liquid layer is much more continuous in the closed pore system than in the open one. This difference results from the fact that atoms in the closed system are not allowed to desorb and leave the pore. Thus melting is initiated by promoting the adsorbed atoms to the second layer. As a consequence, vacancies are formed in the first layer. The melting starts around them and progresses until the number of vacancies is large enough to make the whole layer

melted. This observation proves the importance of the vacancy formation in the melting mechanism in pores, similar to melting on plane surfaces [11, 12]. Another important observation was that the melting of the monolayer did not show any sign of hysteresis. This means that the mechanism of melting in confined geometries is different from that in 3D systems where it is expected to be of the first order type because of the important symmetry difference between crystal and liquid phase.

The GCMC simulation repeated along several isotherms allowed us to calculate a phase diagram of the krypton adsorbed in smooth wall cylindrical pore (Fig. 3). This phase diagram includes a 2D gas phase, monolayer phase and solid 3D phase (above the capillary condensation pressure). The melting transition within monolayer is observed in the range of a few degrees ( $\sim 75$ – $80$  K), depending on the pressure of the external gas. This value is much lower than the melting temperature in a totally filled pore, above the capillary condensation ( $\sim 90$  K [13]). This indicates that the mechanism of melting is different in both situations. Obviously, the existence of the neighbouring layers may modify the thermodynamic properties of the confined system. Some aspects of this effect are discussed below in the case of Kr adsorption in carbon nanotube.

### 3. Melting of a layer in corrugated pores

Figure 4 presents characteristic isotherms of krypton in carbon nanopores, at temperatures ranging between 90 K and 130 K. Although the overall character of adsorption changes with temperature, the adsorption isotherms remain of a stepwise type up to 130 K. There is always the first and the second layer formation before the pore is filled in the process of capillary condensation. This situation allowed us to study melting properties of the first layer as a function of the total loading in the pore, up to the capillary condensation. As will be seen below, the second layer adsorption has a pronounced influence on the properties of the first one.

Figure 5 presents the evolution of the order parameter within the first adsorbed layer along the same isotherms as on Figure 4. At 90 K the adsorbed krypton layer is solid over the whole range of pressures. There is a small increase of the order parameter when the second layer is adsorbed and then when the pore is completely filled due to the capillary condensation. Such an evolution seems quite natural: each next layer stabilizes the previous ones hence the total stability of the confined system increases.

Above  $\sim 95$  K the first layer is fluid. However, its state depends strongly on the external pressure, i.e., on the loading of atoms in the pore. The variation of the order parameter suggests a continuous solidification of the first layer as a function of the external gas pressure. This very peculiar ‘re-entrant’ transition is observed between ca. 95 K and 110 K. At these temperatures the first layer (solid at 90 K) melts but it solidifies when the second layer is adsorbed. Above 130 K the situation changes once again: the second layer does not induce any solidification of the first layer, and only the capillary condensation makes it solid again.

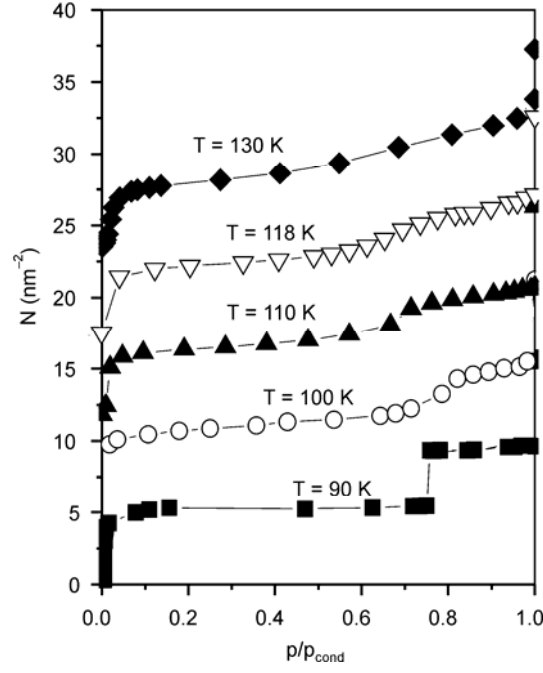


Fig. 4. Adsorption isotherms of Kr in a carbon nanotube. The mean number of adsorbed atoms is drawn as a function of the reduced pressure  $p/p_{\text{cond}}$ , as in Fig. 1. The pressures of the capillary condensation are :  $p_{\text{cond}}(90 \text{ K}) = 6.4 \text{ mbar}$ ,  $p_{\text{cond}}(100 \text{ K}) = 28 \text{ mbar}$ ,  $p_{\text{cond}}(110 \text{ K}) = 105 \text{ mbar}$ ,  $p_{\text{cond}}(118 \text{ K}) = 250 \text{ mbar}$ ,  $p_{\text{cond}}(130 \text{ K}) = 730 \text{ mbar}$

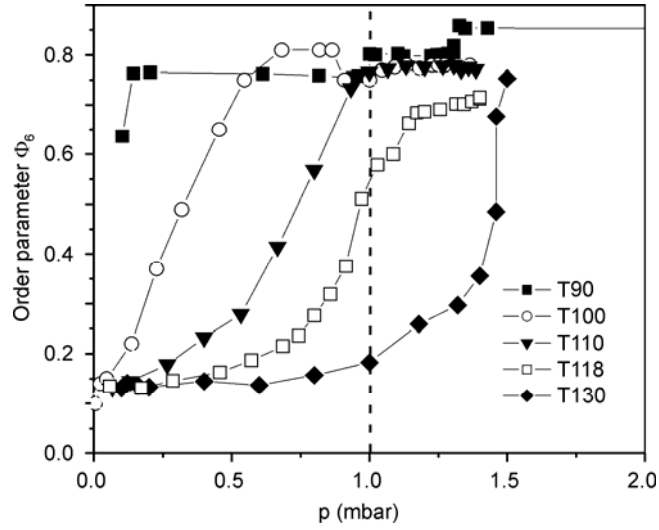


Fig. 5. Order parameter  $\Phi_6$  of Kr monolayer in open-ended carbon nanotube (grand canonical MC simulations)

It is worth remembering that the bulk 3D triple point for Kr atoms appears at ca. 118 K. The results presented above prove that the melting temperature may be either decreased or increased in a confined system. The key factor that determines the temperature and the mechanism of transformation is the strength of the wall–atom interaction. However, geometrical constraints play an important (albeit more subtle) role as well. An interesting illustration of this conclusion can be observed in Figure 5 for  $T = 100$  K. In this case the order parameter in the first layer reaches its maximum in the absence of the second one. However, when the second layer begins to be adsorbed, the order in the first layer slightly decreases. This subtle effect is a consequence of the geometry (size and form) of the pore which defines the mean interatomic distance, i.e., the structure in each layer. A priori, if there is a mismatch between the mean interatomic distance imposed by the pore and the interatomic distance in the bulk solid, adsorption of the second layer may impose a slight deformation of the first one. The whole adsorbed system reaches a more stable configuration when the first layer structure is different from the one that could be expected from the atom–wall interaction only. This is the case of Kr adsorbed in a graphitic nanotube of 4 nm diameter, at 100 K. At higher temperatures, due to the entropy factor, the first layer is already more disordered and a small influence of the second layer is not seen in the order parameter.

#### 4. Conclusions

The simulations of Kr in two types of nanometric cylindrical pores showed that the confined geometry modifies the thermodynamic and structural properties of the adsorbed layers. The shape of the pore and its volume impose geometrical constraints which destabilize the adsorbed system with respect to the 3D bulk material. As a consequence, the effect generally leads to a lower melting temperature in confinement than in the bulk.

The system remains always very heterogeneous: the properties of each adsorbed layer depend on its distance from the pore wall. In particular, the mechanism of melting transition is different in each layer and, additionally, it varies with the amount of atoms adsorbed in the pore. This observation, very interesting from the point of view of basic science, has also important practical consequences in the case of nanopores where only few layers are adsorbed.

Another important factor is the strength of the atom–wall interaction. As could be clearly seen from the presented results, it affects particularly the properties of the first few layers next to the pore wall. When only one layer is adsorbed, its melting temperature is even lower than that in a totally filled pore. When the following layer is built, its presence affects the mechanism of melting of the first one. Depending on the strength and corrugation of the atom–wall interaction the influence of the interface between the adsorbed system and the walls may be extended up to the layers more distant from the pore wall. Consequently, melting is a complicated succession of transitions where different layers melt at different temperatures.



## References

- [1] BATCHELOR R.W., FOSTER A.G., Trans. Faraday Soc., 40 (1944), 300.
- [2] GELB L.D., GUBBINS K.E., RADHAKRISHNAN R., SLIWINSKA-BARTKOWIAK M., Rep. Prog. Phys., 62 (1999), 1573.
- [3] SLIWINSKA-BARTKOWIAK M., DUDZIAK G., SIKORSKI R., GRAS R., RADHAKRISHNAN R., GUBBINS K.E., J. Chem. Phys., 114 (2001), 950.
- [4] MADDOX M.W., GUBBINS K.E., J. Chem. Phys., 107 (1997), 9659.
- [5] MIYAHARA M., GUBBINS K.E., J. Chem. Phys., 106 (1997), 2865.
- [6] RADHAKRISHNAN R., GUBBINS K.E., SLIWINSKA-BARTKOWIAK M., J. Chem. Phys., 112 (2000), 11048.
- [7] DOMINGUEZ H., ALLEN M.P., EVANS R., Mol. Phys., 96 (1999), 209.
- [8] RADHAKRISHNAN R., GUBBINS K.E., Phys. Rev. Lett., 79 (1997), 2847.
- [9] MERMIN N.D., Phys. Rev., 176 (1968), 250.
- [10] KUCHTA B., LLEWELLYN P., DENOYEL R., FIRLEJ L., Coll. Surfaces A, 241 (2004), 137.
- [11] FIRLEJ L., KUCHTA B., ETTERS R., PRZYDRÓŻNY W., FLENNER E., J. Low Temp. Phys., 122 (2001), 171.
- [12] ETTERS R., FLENNER E., KUCHTA B., FIRLEJ L., PRZYDROZNY W., J. Low Temp. Phys., 122 (2001), 121.
- [13] KUCHTA B., LLEWELLYN P., DENOYEL R., FIRLEJ L., Coll. Surfaces, A241 (2004), 137.

*Received 15 April 2005*

*Revised 6 December 2005*